

Measurement of the thermal properties of gadolinium and dysprosium titanate

Byung-Ho Lee^{a,*}, Han-Soo Kim^a, Sang-Hyun Lee^b, Dong-Seong Sohn^a

^a Korea Atomic Energy Research Institute, P.O. Box 105, Yuseong, Daejeon 305-600, South Korea

^b Korea Research Institute of Standards and Science, P.O. Box 102, Yuseong, Daejeon 305-600, South Korea

Available online 9 December 2006

Abstract

Gadolinium titanate ($Gd_xTi_yO_z$) and dysprosium titanate ($Dy_xTi_yO_z$) have been developed as burnable poison and neutron absorbing materials in nuclear application, respectively. They have high neutron absorption capability and unique neutron absorption efficiency. Since their thermal properties have not been well established as yet, their specific heat capacity and thermal diffusivity were measured and they were used to derive the thermal conductivity for the $Gd_xTi_yO_z$ and $Dy_xTi_yO_z$ with various compositions from room temperature to 1000 °C. We also investigated the effect of the sintering temperature on the thermal properties. Although they are chemically and physically similar, the trend of the thermal conductivity of $Gd_xTi_yO_z$ and $Dy_xTi_yO_z$ differed significantly. The measured thermal properties can be used for the safety and performance analysis which includes the precise temperature calculation for irradiation test and for the design for nuclear application.

© 2006 Elsevier B.V. All rights reserved.

Keywords: Gadolinium titanate; Dysprosium titanate; Neutron absorbing element; Thermal properties

1. Introduction

Gadolinium titanate ($Gd_xTi_yO_z$) and dysprosium titanate ($Dy_xTi_yO_z$) have been developed as burnable poison and neutron absorbing materials, respectively. They have high initial neutron absorbing capability and unique neutron absorption efficiency with good irradiation resistance [1].

In particular, $Dy_xTi_yO_z$ has been used as control rod material in the VVER-1000 reactors as well as in research reactors in Russia [2]. $Dy_xTi_yO_z$ is superior to the conventional neutron absorbing materials such as B_4C and Ag–In–Cd since $Dy_xTi_yO_z$ has good irradiation resistance with a lower swelling rate under irradiation and it sustains the capability of absorbing neutrons during irradiation. $Gd_xTi_yO_z$ is considered as good burnable poison material to control an excessive reactivity, provide a safety shutdown margin, and compensate for a reducing reactivity.

However, their thermal properties have not been well established as yet for an analysis of their thermal performance under irradiation although the thermal properties are the prerequisite to determine the temperature distribution [3].

In this regard, we investigated the thermal behavior for $Gd_xTi_yO_z$ and $Dy_xTi_yO_z$ such as their heat capacity and thermal diffusivity up to a temperature of 1000 °C. The effect of the sintering temperature on the thermal properties was also examined. Consequently, the thermal conductivities derived from the measured specific heat capacity and thermal diffusivity were estimated to clarify the effects of the contents of the neutron absorption elements and the sintering temperatures.

2. Experimental

2.1. Sample preparation

The samples of $Gd_xTi_yO_z$ and $Dy_xTi_yO_z$ were fabricated by accurately controlling the contents of gadolinium and dysprosium, respectively.

Dy_2O_3 and TiO_2 powders were prepared for the fabrication of a $Dy_xTi_yO_z$ pellet. The mixing ratio was determined for containing the precise dysprosium composition in the pellets. Both powders were mixed well in a tubular mixer and then milled in a zirconia crucible by using a planetary mill. The green pellet was fabricated by hydraulically pressing the mixed powder to 300 MPa. Based on the TMA sinterability scoping tests, the green pellets were sintered at the temperatures of 1600 and 1650 °C in air [4].

* Corresponding author. Tel.: +82 42 868 8984; fax: +82 42 864 1089.
E-mail address: bholee@kaeri.re.kr (B.-H. Lee).

Table 1

The specimens for the thermal property measurements of $Gd_xTi_yO_z$ and $Dy_xTi_yO_z$

Designation	Compositions (mol%)		Density (g/cm ³)
	Gd ₂ O ₃	TiO ₂	
Gd20A ^a	15.8	84.2	5.25
Gd20B ^b	15.8	84.2	5.28
Gd42C ^c	45.8	54.2	6.31
Gd42D ^d	45.8	54.2	6.34
Gd47C ^c	56.4	43.6	6.57
Gd47D ^d	56.4	43.6	6.55
GdHC ^c	50.0	50.0	6.23
GdHD ^d	50.0	50.0	6.24

Designation	Compositions (mol%)		Density (g/cm ³)
	Dy ₂ O ₃	TiO ₂	
Dy40C ^c	39.1	60.9	6.70
Dy40D ^d	39.1	60.9	6.86
DyHC ^c	50.0	50.0	6.79
DyHD ^d	50.0	50.0	6.93

^a The sintering temperature of 1400 °C.

^b The sintering temperature of 1450 °C.

^c The sintering temperature of 1600 °C.

^d The sintering temperature of 1650 °C.

The $Gd_xTi_yO_z$ pellets were fabricated by similar procedures to those of the $Dy_xTi_yO_z$. Appropriate ratios of powders were mixed into different compositions, ranging from 2.0 to 4.7 g Gd/cm³. The sintering temperature was also the same except for the $Gd_xTi_yO_z$ samples with the gadolinium contents of 2.0 g Gd/cm³. $Gd_xTi_yO_z$ with 2.0 g Gd/cm³ was sintered at the temperature of 1400 and 1450 °C since they have a melting temperature of 1545 °C. Bulk densities of the pellets were measured by the immersion method.

The samples were cut into disk shapes for their heat capacity and thermal diffusivity measurements. The chemical compositions, densities and identifications are summarized in Table 1. The identifications are referred to on the basis of the sintering temperature and the contents of gadolinium (g Gd/cm³) and dysprosium (g Dy/cm³) in the sample disks. For example, Gd20A denotes the sample manufactured with the gadolinium content of 2.0 g Gd/cm³ at the sintering temperature of 1400 °C. The specimen designations with “H” indicate that the specimens have the 1:1 composition of lanthanide oxide (Gd₂O₃ or Dy₂O₃) and TiO₂.

2.2. Thermal property measurements

For the proper and accurate thermal property measurements, disks of 5 mm in diameter with 2 mm thickness were used for the heat capacity and those of 10 mm in diameter with 1 mm thickness for the thermal diffusivity. The thermal properties were measured from room temperature to 1000 °C.

Specific heat capacity was measured by DSC Netzsch 404C in an inert atmosphere. The measurements were performed at an interval of 50 °C. Heating rate was 10 °C/min. The inert atmo-

sphere was obtained by nitrogen gas with a purity of 99.999% and its flow rate was 50 ml/min. The accuracy of the measurements was confirmed by using synthetic sapphire, NIST SRM 720, as a reference sample to be within ±2.0% of the entire measuring temperature range.

Thermal diffusivity measurements were made by means of a laser flash apparatus, SINKU-RIKO (TC-7000VH/L). All the measurements were carried out in a vacuum at a pressure less than 4×10^{-4} Pa. The laser flash system was checked by poco-graphite (SRM 8245, NIST) and the accuracy was ±3%. Thermal diffusivity was analyzed in half time using Parker method. The pulse time of laser was estimated about (0.9 ± 0.1) ms. The results were calculated using half time of maximum temperature increase on the back of the sample for the thermal diffusivity. Thermal diffusivity data was corrected by Azumi and Takahashi's method to reduce the effect of finite pulse. The temperature measurement of the back of the sample was conducted using In–Sb infrared sensor. For consistent heating energy on samples, the front and the back of samples were covered with a thin graphite layer. The mean value of five measurements of thermal diffusivity was computed for thermal diffusivity.

3. Results and discussion

3.1. Specific heat capacity measurement

The specific heat capacities of $Gd_xTi_yO_z$ and $Dy_xTi_yO_z$ were measured from room temperature up to 1000 °C. The measured specific heat capacity is displayed in Fig. 1 for $Gd_xTi_yO_z$ and in Fig. 2 for $Dy_xTi_yO_z$. The measured specific heat capacity data was fitted to the following polynomial for the temperature by using the least-square method:

$$c_p(T)/(J/g \text{ } ^\circ\text{C}) = a_0 + a_1T + a_2T^2 + a_3T^3 + a_4T^4 \quad (1)$$

where c_p is in J/g °C and T is in Celsius. Their coefficients are listed in Table 2.

The specific heat capacity of $Gd_xTi_yO_z$ increases with the temperature without anomaly as shown in Fig. 1. The gadolinium contents have a considerable effect on the specific heat capac-

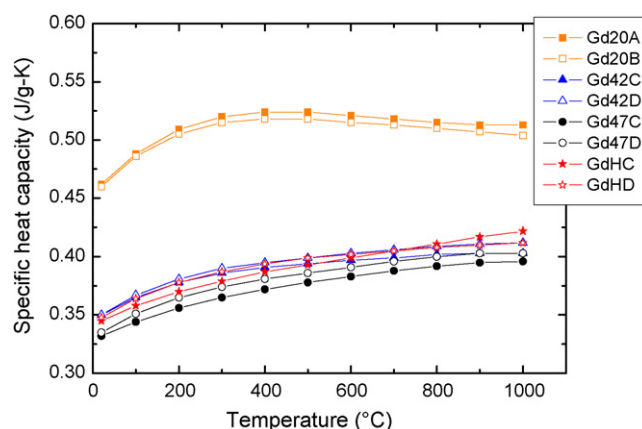


Fig. 1. The specific heat of $Gd_xTi_yO_z$ with various gadolinium contents up to 1000 °C.

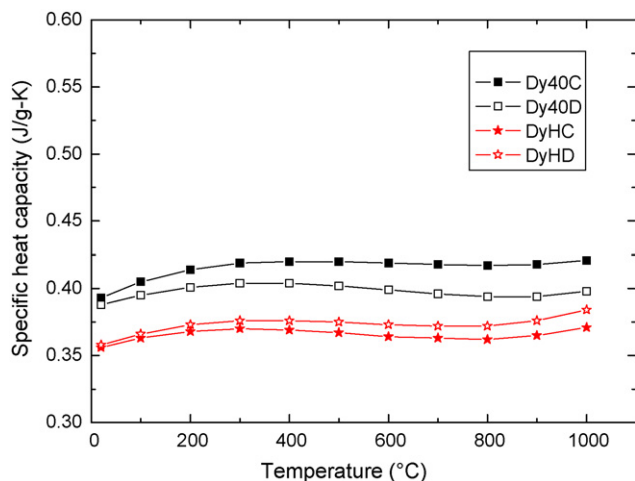


Fig. 2. The specific heat of $Dy_xTi_yO_z$ up to 1000 °C.

ity so that the specific heat capacity decreases by increasing the content of gadolinium. The $Gd_xTi_yO_z$ with decreasing gadolinium content has a larger fraction of TiO_2 . Since the TiO_2 has a higher specific heat capacity than Gd_2O_3 , $Gd_xTi_yO_z$ with low content of gadolinium is higher than that with high content of gadolinium. The specific heat capacities of Gd42, Gd47 and GdH cannot be discernable since there seems to be no significant difference in the gadolinium content. It can be seen that the sintering temperature has a negligible effect on the specific heat capacity.

The specific heat capacity of $Dy_xTi_yO_z$ is significantly different from that of $Gd_xTi_yO_z$ as shown in Fig. 2. The specific heat capacity increases with the temperature and then it remains constant or decreases after 300 °C slightly. The specific heat capacity increases again at a temperature above 800 °C. The specific heat capacity is higher in the non-stoichiometric $Dy_xTi_yO_z$ than in the stoichiometric $Dy_2Ti_5O_z$ due to the higher content of TiO_2 in the former. Similar to $Gd_xTi_yO_z$, there is no dependency of the specific heat capacity of $Dy_xTi_yO_z$ on the sintering temperature at the low temperature but the different sintering temperature results to a different specific heat capacity at the high temperature.

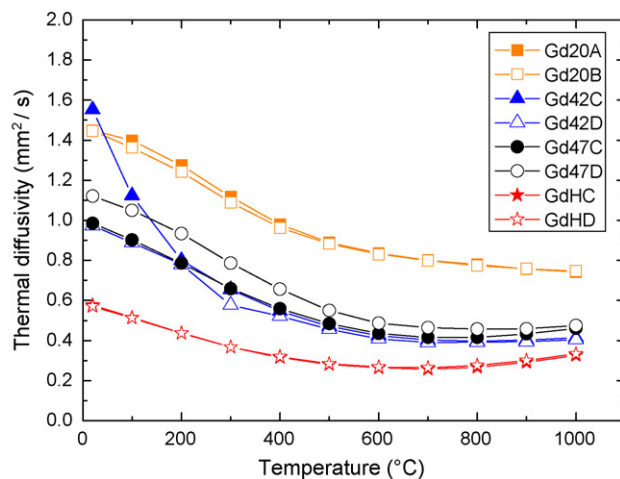


Fig. 3. Thermal diffusivity of $Gd_xTi_yO_z$ with various gadolinium contents up to 1000 °C.

3.2. Thermal diffusivity measurement

The thermal diffusivity was measured for $Gd_xTi_yO_z$ and $Dy_xTi_yO_z$ from room temperature up to 1000 °C. In particular, the effect of the gadolinium content on the thermal diffusivity was investigated for $Gd_xTi_yO_z$. We also examined the effect of the sintering temperature on the thermal diffusivity.

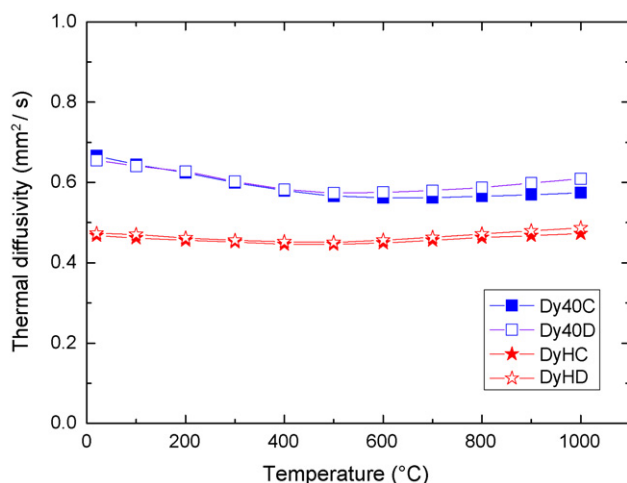
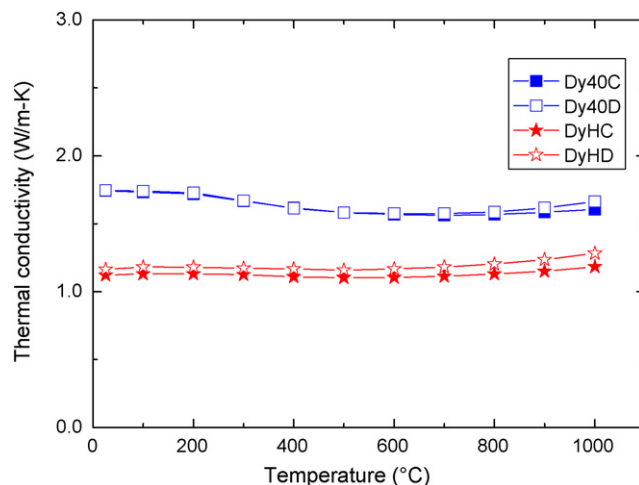
The variation of the thermal diffusivity measured for $Gd_xTi_yO_z$ is shown in Fig. 3 and for $Dy_xTi_yO_z$ in Fig. 4. Fig. 3 illustrates that the thermal diffusivity of $Gd_xTi_yO_z$ decreases with the temperature and it is not affected by the different sintering temperatures. The specimen with the lowest gadolinium content shows the highest thermal diffusivity than the others. The stoichiometric $Gd_2Ti_5O_z$ (GdH) has the lowest thermal diffusivity although its content of gadolinium lies between Gd42 and Gd47.

Fig. 4 illustrates that the thermal diffusivity of $Dy_xTi_yO_z$ decreases with the temperature up to 500 °C and then it increases slightly up to 1000 °C. The non-stoichiometric $Dy_xTi_yO_z$ (Dy40) has higher thermal diffusivity than the stoichiometric $Dy_2Ti_5O_z$ (DyH). The sintering temperature does not affect the thermal diffusivity.

Table 2

The coefficients of the fitted specific heat capacity

	a_0	$a_1 (\times 10^4 \text{ } ^\circ\text{C}^{-1})$	$a_2 (\times 10^7 \text{ } ^\circ\text{C}^{-2})$	$a_3 (\times 10^{10} \text{ } ^\circ\text{C}^{-3})$	$a_4 (\times 10^{13} \text{ } ^\circ\text{C}^{-4})$
Gd20A	0.454	4.167	-8.372	6.552	-1.759
Gd20B	0.453	4.170	-9.274	8.552	-2.938
Gd42C	0.346	2.326	-4.518	4.451	-1.688
Gd42D	0.345	2.649	-5.297	5.370	-2.051
Gd47C	0.328	1.963	-3.426	3.819	-1.679
Gd47D	0.330	2.587	-5.157	5.656	-2.349
GdHC	0.341	1.892	-2.864	2.809	-1.028
GdHD	0.344	2.390	-4.039	3.498	-1.163
Dy40C	0.390	1.817	-3.621	2.662	-0.546
Dy40D	0.386	1.109	-1.830	0.178	0.662
DyHC	0.353	1.196	-2.613	1.479	0.119
DyHD	0.355	1.370	-2.705	1.355	0.270

Fig. 4. Thermal diffusivity of $Dy_xTi_yO_z$ up to 1000 °C.Fig. 6. Thermal conductivity of $Dy_xTi_yO_z$ up to 1000 °C.

3.3. Thermal conductivity estimation

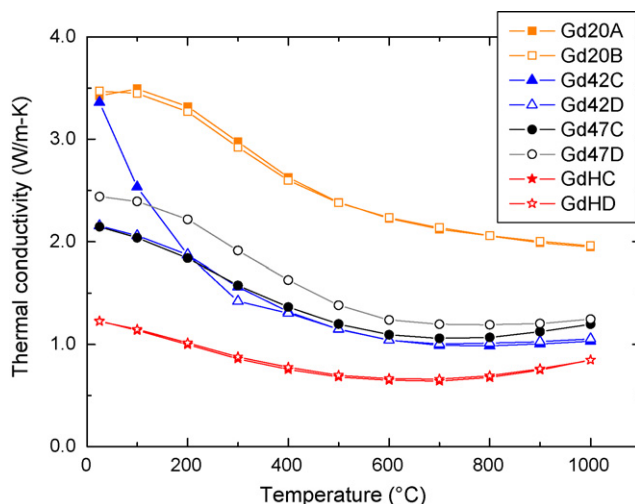
The thermal conductivities of $Gd_xTi_yO_z$ and $Dy_xTi_yO_z$ were obtained from the measured values of the thermal diffusivity, specific heat capacity and density such as:

$$\lambda = \alpha c_p \rho \quad (2)$$

where α is the thermal diffusivity (m^2/s), c_p the specific heat capacity ($J/kg\ K$), and ρ is the density (kg/m^3). The calculated thermal conductivity is shown in Fig. 5 for $Gd_xTi_yO_z$ and in Fig. 6 for $Dy_xTi_yO_z$.

Fig. 5 illustrates that the thermal conductivity of $Gd_xTi_yO_z$, in general, decreases with the temperature and then it remains almost constant up to a temperature of 1000 °C for the non-stoichiometric $Gd_xTi_yO_z$. In the case of stoichiometric Gd_2TiO_5 (GdH), the thermal conductivity increases distinctly at the temperature region higher than 600 °C.

The thermal conductivity is highest in the specimen (Gd20) with the lowest gadolinium content of 2.0 g Gd/cm³, whereas it

Fig. 5. Thermal conductivity of $Gd_xTi_yO_z$ with various gadolinium contents up to 1000 °C.

is lowest in the stoichiometric Gd_2TiO_5 (GdH). This means that the gadolinium content and stoichiometry reduce the thermal conductivity. There is no discernable difference between Gd42 and Gd47 due to the small difference in the gadolinium content. It is evident that there is no significant sintering temperature effect on the thermal conductivity.

Fig. 6 illustrates the thermal conductivity of non-stoichiometric $Dy_xTi_yO_z$. The thermal conductivity of non-stoichiometric $Dy_xTi_yO_z$ (Dy40) decreases slightly with the temperature, whereas the stoichiometric Dy_2TiO_5 (DyH) increases a little with the temperature. Their thermal conductivities can approximate from 1.0 to 1.75 W/m K. The thermal conductivity of $Dy_xTi_yO_z$ is not influenced by the sintering temperature considerably.

The constant thermal conductivity or a slight increase in the thermal conductivity at the high temperature is due to the dominant contribution of an electronic conduction to the thermal conductivity in $Dy_xTi_yO_z$. When the trend of thermal conductivity is compared between $Dy_xTi_yO_z$ and $Gd_xTi_yO_z$, the electronic conduction term appears stronger in $Dy_xTi_yO_z$ than in $Gd_xTi_yO_z$.

It is also remarkable that the stoichiometric lanthanides such as Gd_2TiO_5 and Dy_2TiO_5 have a better resistance to a neutron irradiation [2] but they have a far worse thermal conductivity than the non-stoichiometric lanthanides.

4. Conclusions

To investigate the thermal properties of $Gd_xTi_yO_z$ and $Dy_xTi_yO_z$, the specific heat capacity and thermal diffusivity were measured by the DSC and laser flash method, respectively. The thermal properties were determined from room temperature to 1000 °C for $Gd_xTi_yO_z$ and $Dy_xTi_yO_z$ with various contents of neutron absorbing elements (gadolinium and dysprosium) and different sintering temperatures. The thermal conductivities derived from the specific heat capacity and thermal diffusivity reveals that:

- The increase in the content of gadolinium and dysprosium reduces the thermal conductivity.

- Thermal conductivity for all the $Gd_xTi_yO_z$ and the non-stoichiometric $Dy_xTi_yO_z$ decreases with the temperature, whereas the stoichiometric Dy_2TiO_5 increases slightly.
- The sintering temperature does not affect the thermal conductivity for $Gd_xTi_yO_z$ and $Dy_xTi_yO_z$.
- The stoichiometric Gd_2TiO_5 and Dy_2TiO_5 have the lowest thermal conductivity when compared to the other non-stoichiometric $Gd_xTi_yO_z$ and $Dy_xTi_yO_z$.

References

- [1] G. Panneerselvam, R.V. Krishnan, M.P. Antony, K. Nagarajan, T. Vasudevan, P.R.V. Rao, *J. Nucl. Mater.* 327 (2004) 220.
- [2] V.D. Risovany, E.E. Varlashova, D.N. Suslov, *J. Nucl. Mater.* 281 (2000) 84.
- [3] W. Wiesenack, B.H. Lee, D.S. Sohn, *Nucl. Eng. Technol.* 37 (2005) 317.
- [4] H.S. Kim, C.Y. Joung, S.H. Kim, B.H. Lee, Y.W. Lee, D.S. Sohn, S.H. Lee, *J. Kor. Ceram. Soc.* 39 (2002) 1108.